Comparison of 3D and 2D Li Diffusion in Cubic and Hexagonal $Li_x TiS_2$ – A Study by Solid State ^{7}Li NMR Methods

Martin Wilkening and Paul Heitjans

Leibniz Universität Hannover,
Institut für Physikalische Chemie und Elektrochemie, and
Zentrum für Festkörperchemie und Neue Materialien,
Callinstr. 3-3a, D-30167 Hannover, Germany

E-Mail: wilkening @pci.uni-hannover.de; heitjans@pci.uni-hannover.de

Dedicated to Professor Hermann Schmalzried on the occasion of his 75th birthday.

Abstract

Li diffusion in spinel-type structured cubic and hexagonal $Li_x TiS_2$ with $x = 0.6$ and 0.7, respectively, was investigated by solid state NMR spectroscopy. In layered hexagonal $Li_x TiS_2$, Li diffusion is known to be confined to the van-der-Waals gap between the TiS_2 planes, *i. e.*, it is two-dimensional (2D). In cubic $Li_x TiS_2$, however, Li diffusion takes place in the three-dimensional (3D) interstitial space formed by the TiS_6-polyhedra. Both polymorphs form a unique pair for studying the effects of dimensionality on Li diffusion within a host structure of the same chemical composition. ^{7}Li spin-alignment echo and spin-lattice relaxation NMR methods were applied to measure Li jump rates. Additionally, solid echo NMR spectroscopy was used to estimate the Li diffusivity in cubic $Li_{0.6} TiS_2$. The activation energies for Li jumps in the two materials are very similar. Nevertheless, Li diffusion in the 3D host is slower than in the layered modification by a factor of about ten.

Keywords

Li diffusion, dimensionality, solid state NMR, spin-lattice relaxation, spin-alignment echo, ultraslow motion, cubic $Li_x TiS_2$

1 Introduction

Layered hexagonal titanium disulfide, *h*-TiS_2, is known to be a highly suitable host material for the accommodation of small ions like Li^+ or Na^+, see, *e. g.*, Refs. [1-3]. Lithium ions can be easily inserted into the van-der-Waals gap between the TiS_2 layers electrochemically or chemically by treatment with *n*-butyl lithium [1,2]. Monophase $Li_x TiS_2$ (CdI$_2$-type structure, space group $P\bar{3}m1$) is stable in the whole intercalation range $0 < x \le 1$. With increasing Li content the c-axis and slightly also the a-axis enlarge whereas the layered structure of the host material stays unchanged [1]. Li diffusion in $Li_x TiS_2$ is two-dimensional as was unambiguously confirmed previously by our group using frequency dependent NMR spin-lattice relaxation (SLR) measurements performed

in the laboratory as well as in the rotating frame [4]. Layered Li_xTiS_2 is one of only few examples, see, *e. g.*, the ^{1}H NMR study of Conradi and co-workers [5], where 2D diffusion of small cations was clearly probed by the frequency dependence of the NMR spin-lattice relaxation rate. Hexagonal $LiTiS_2$ is well-known as an excellent electrode material for secondary Li ion batteries due to the high cycleability and Li diffusivity as well as the good electronic conductivity [6,7]. At ambient temperature the Li jump rate τ^{-1} is about $10^6 \, s^{-1}$ which corresponds to a Li self-diffusion coefficient $D_{Li} = r^2/4\tau$ of roughly $10^{-14} \, m^2 s^{-1}$, see Ref. [8]. r is the jump distance.

In addition to the layered host, a cubic polymorph of titanium sulfide with the same chemical formula does exist [9,10]. Spinel-type cubic Li_xTiS_2 (space group $Fd\bar{3}m$) was first prepared by Schöllhorn and Payer after electrochemically removing Cu from the corresponding spinel $CuTi_2S_4$ [9]. Similarly to the hexagonal polymorph, Li insertion into cubic TiS_2 can easily be achieved up to the composition $Li_{x=1.0}TiS_2$ by treating the powder sample with *n*-butyl lithium. As in the case of layered TiS_2 the topotactic intercalation process is reversible. Cubic Li_xTiS_2 is single-phase. The partial molar free energy for the uptake of one equivalent of Li is similar for both modifications [9]. During intercalation the cubic material undergoes an isotropic expansion. Its advantage over the layered modification is that solvent co-intercalation on extended cycling in a secondary ion battery is precluded due to the framework structure of cubic Li_xTiS_2. It is metastable up to a temperature T of about 700 K. At higher T it transforms irreversibly into the thermodynamically stable hexagonal modification.

In the present paper we will use various ^{7}Li NMR techniques to probe the Li diffusivity in cubic $Li_{0.6}TiS_2$. The results will be compared with those which we have obtained for hexagonal $Li_{0.7}TiS_2$, recently, see Ref. [11]. In [11] we have measured a solitary Li diffusion process in hexagonal $Li_{0.7}TiS_2$ by means of various ^{7}Li NMR methods over a dynamic range of about ten decades. Whereas in hexagonal Li_xTiS_2 cation diffusion is confined to the van-der-Waals gap, *i. e.*, it is two-dimensional, in the cubic polymorph the Li ions make use of all three dimensions while jumping. Both polymorphs form a unique pair, which can be used to study the effects of dimensionality on Li diffusion within a host structure of the same chemical composition.

2 Experimental

2.1 Sample preparation

The samples had been prepared by Payer and Schöllhorn and were used for ^{7}Li relaxation NMR studies [4] by our group before. For layered TiS_2, titanium and sulphur powders of high purity were mixed in the ratio 1:2.1 and then placed in an evacuated quartz tube. The mixture was heated at 870 K for about two weeks. Excess sulphur was removed at 420 K under vacuum. The starting compound to prepare cubic TiS_2 is the copper thiospinel $CuTi_2S_4$. To obtain the pure cubic binary phase, Cu was removed from the spinel framework by reaction with Br_2 in acetonitrile. In both samples Li was intercalated chemically at room temperature using a 0.3 molar solution of *n*-butyl lithium in hexane.

2.2 NMR setup

For the ^{7}Li solid state NMR experiments a modified Bruker MSL 100 and an MSL 400 spectrometer were used. Corresponding to the magnetic fields of 4.7 and 9.4 T the [7]Li resonance frequency was either 77.7 MHz or 155.5 MHz. The 90° pulse length was about 5 μs in both cases. The spin-lattice relaxation rates shown here were mostly taken from Refs. [4,11,12]. The standard saturation recovery rf pulse sequence was used to record spin-lattice relaxation rates $1/T_1$ in the laboratory frame [13]. Spin-lattice relaxation data in the rotating frame were acquired using the spin-lock technique introduced by Redfield [14] which was first applied by Ailion et al. [15] and Look et al. [16]. Solid echo spectra were measured using the two-pulse sequence, $90° - t_e - 64°$, with an interpulse delay t_e of 20 μs. [7]Li spin-alignment echoes, see, $e. g.$, Refs. [11,17,18], as a function of mixing time t_m and for fixed evolution time t_p were monitored by means of the Jeener-Broekaert three-pulse sequence [19]: $90° - t_p - 45° - t_m - 45°$. A suitable phase cycling [20] was chosen in order to reduce pulse imperfections and to suppress unwanted magnetization in the alignment echo which shows up after the last 45° pulse. The mixing time t_m was varied from 100 μs up to 10 s.

3   Results and discussion

3.1 Solid echo NMR spectra

First insights into Li diffusion in c-Li$_{0.7}$TiS$_2$ are obtained by recording static ^{7}Li NMR spectra between $T = 160$ K and 433 K (Fig. 1). In the rigid lattice regime, $i. e.$, below about 230 K, the spectrum is composed of a dipolarly broadened central transition and satellite intensities which are due to the interaction of the quadrupole moment of the [7]Li nucleus with a non-vanishing electric field gradient at the nuclear site. In c-Li$_x$TiS$_2$ the Li$^+$ cations reside preferentially in polyhedra with distorted octahedral symmetry. The quadrupole splitting, $i. e.$, the frequency distance between the inner satellite lines, is about 13 kHz which, in the case of a spin-3/2 nucleus like [7]Li exposed to an axially symmetric field gradient, results in a quadrupole coupling constant of about 26 kHz at 160 K. Interestingly, the central line exhibits a chemical anisotropy $\Delta\sigma$. Simulation of the static line shape using the WinSolids software [21] yields $\Delta\sigma = 25(1)$ ppm. Similar results were found by Prigge and Müller-Warmuth [22]. With increasing Li diffusivity the dipolar and quadrupolar interactions as well as those due to chemical shift anisotropy are averaged. At about 350 K the quadrupole powder pattern has completely disappeared and $\Delta\sigma = 0$ is found. Averaging of quadrupole interactions is expected when the Li jump rate is several times larger than the quadrupolar splitting. Thus, at about 350 K a jump rate of the order of 10^5 s^{-1} can be estimated. The rigid-lattice spectra of the layered modification of Li$_x$TiS$_2$ (with $0 < x < 1$) are similar to those of the cubic form [22, 23]. However, in contrast to the case of 3D diffusion in c-Li$_x$TiS$_2$, quadrupole interactions and the asymmetry of the central line are not averaged with increasing T because Li diffusion is confined to two dimensions. The van-der-Waals gap between the TiS$_2$ planes of hexagonal Li$_x$TiS$_2$ contains only two different Li sites, octahedral and tetrahedral ones. Thus, diffusion in hexagonal Li$_x$TiS$_2$ is highly anisotropic, and complete averaging of electric and magnetic interactions seems to be not possible even at very high temperatures, see also Ref. [22].
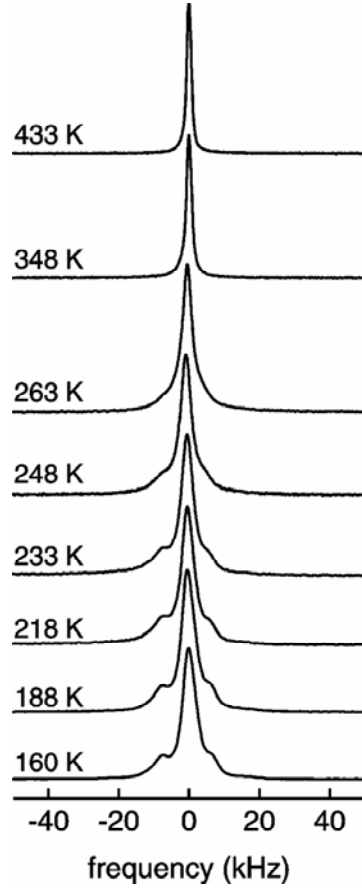
Fig. 1: Static ^{7}Li NMR spectra of cubic Li$_x$TiS$_2$ recorded at 77.8 MHz for various temperatures (160 K – 433 K). In the rigid-lattice regime (up to $T \approx 230$ K) the spectra are composed of an asymmetric central line and a quadrupole powder pattern revealing a quadrupole coupling constant of about 26 kHz. Increasing Li diffusivity leads to an averaging of electric and magnetic interactions determining the line shape at low temperatures. A single, motionally narrowed NMR line is observed at about 400 K due to 3D Li diffusion in cubic Li$_x$TiS$_2$.

3.2 Spin-lattice relaxation NMR: laboratory and rotating frame measurements

In addition to the investigation of the temperature dependence of ^{7}Li NMR spectra, the measurement of longitudinal NMR relaxation rates provides further insight into Li diffusion processes [25]. Longitudinal relaxation, *i. e.*, spin-lattice relaxation, can be effectively induced by cation diffusion. The relaxation rate T_1^{-1} is related to the hopping correlation rate τ^{-1} of the nuclei [25,26]. As a function of inverse temperature, $1/T_1$ will show a characteristic diffusion induced maximum whose position on the temperature scale depends on the strength of the applied external magnetic field B_0. At the temperature where the maximum appears, the relation $\omega_0 \tau \approx 1$ holds [26]. ω_0 denotes the angular Larmor frequency which is related to B_0 via $\omega_0 = \gamma B_0$, where γ is the magnetogyric ratio of the nucleus. The temperature dependence of τ^{-1} is normally described by an

4

Arrhenius relation $\tau^{-1} = \tau_0^{-1} \exp\left(-E_A / k_B T\right)$, where τ_0^{-1} is the pre-exponential factor and E_A the activation energy of the diffusion process.
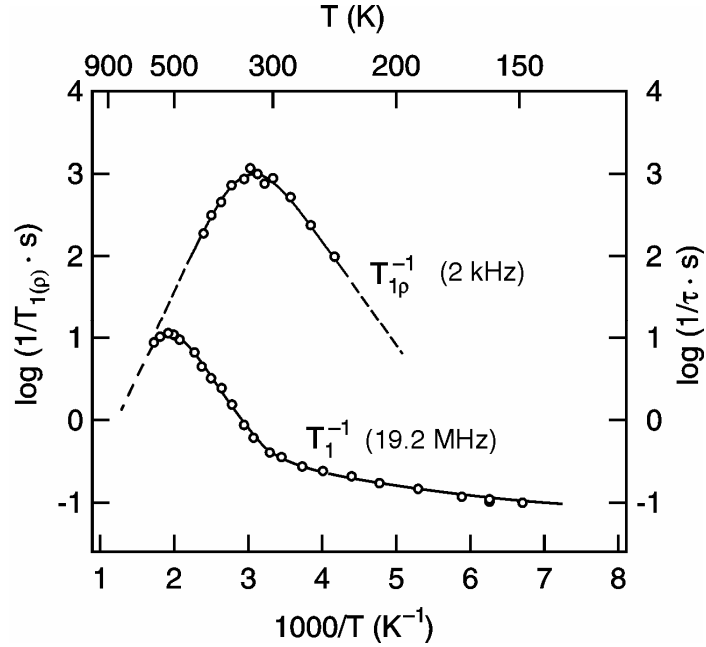
^{7}Li NMR spin-lattice relaxation rates $1/T_1$ of c-Li$_x$TiS$_2$ with $x = 0.6$ were recorded in the laboratory frame at a resonance frequency of $\omega_0 / 2\pi = 19.2$ MHz. They are shown as a function of reciprocal temperature $1/T$ (30 K – 600 K) in Fig. 2 in a double-logarithmic representation. The temperature scale of Fig. 2 can be subdivided into four different ranges. Below 160 K the SLR rates follow a temperature dependence according to a power law $T_1^{-1} \propto T^{\kappa_1}$ with an exponent $\kappa_1 = 0.75(1)$ (range I). At about 160 K the exponent changes, and $\kappa_2 = 1.8(1)$ is found between 160 K and 315 K (range II). SLR induced by coupling of the nuclear spins with conduction electrons or by lattice vibrations would lead to $\kappa_1 = 1$ and to $\kappa_2 = 2$, respectively. However, in the present case the relaxation rate is presumably influenced by an additional contribution due to paramagnetic impurities of the sample. In preparing the sample, complete removal of Cu$^+$ ions can hardly be achieved. Thus, slight deviations from pure electron and phonon induced relaxation behaviour are expected.
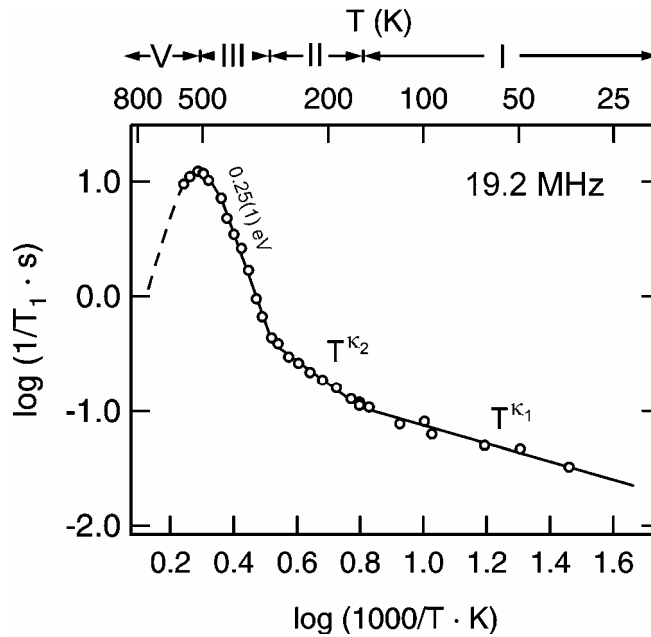
Fig. 2: Temperature dependence of the laboratory frame spin-lattice relaxation rate $1/T_1$ of cubic Li$_x$TiS$_2$ with $x = 0.6$. In ranges I and II the rate follows a weaker-than-activated temperature dependency which can be expressed by two power laws with the exponents κ_1 and κ_2. The flank of the diffusion induced rate maximum shows up above 315 K. Data were taken from Refs. [12,24].

Above 315 K the flank of the diffusion induced rate peak shows up (range III). In this region longitudinal relaxation is mainly induced by thermally activated translational motions of the ^{7}Li nuclei. The slope of the flank corresponds to an activation energy of about 0.25 eV. In order to obtain the pure diffusion induced relaxation rates $T_{1\,\mathrm{diff}}^{-1}$, the background relaxation rates (range I and II) were extrapolated to higher T and subtracted from the overall rate T_1^{-1}. The temperature dependence of $T_{1\,\mathrm{diff}}^{-1}$ between 315 K and 450 K yields an activation energy of 0.29(1) eV, thus somewhat larger than that obtained from the data without background correction. In general, the slope of the low-T relaxation flank corresponds to short-range motions rather than to long-range diffusion [26]. The latter one determines the slope of the corresponding high-temperature flank of the relaxation rate peak. Unfortunately, the high-T flank of the relaxation rate peak is not accessible. As mentioned above, for temperatures higher than 700 K the cubic polymorph of Li$_x$TiS$_2$ transforms irreversibly into the hexagonal modification. Thus, all the NMR experiments had to be restricted to below about 700 K. In contrast to the activation energy deduced from the high-temperature flank, the slope of the low-T flank is additionally influenced by correlation effects due to structural disorder and/or Coulomb interactions of the hopping particles [27-29]. Following these considerations the value of 0.29(1) eV may be interpreted in terms of an apparent activation energy of the Li diffusion process. For comparison, the corresponding activation energy for the hexagonal modification is 0.37(2) eV, thus, somewhat larger than that for the cubic polymorph (*cf.* Fig. 4). However, the value for the layered modification does not seem to be influenced by correlation effects [11] so that the proper activation energies of the cubic and hexagonal modifications appear to be very similar (see below). It is noted that in our previous SLR study [4] only the contribution of range I was used for the background correction, and somewhat smaller activation energies were obtained. Nevertheless the conclusion drawn in [4] that the Li jump rate in the hexagonal modification is higher than that in the cubic one remains valid (see below).

A relatively direct access to microscopic jump rates is given when the maximum of the relaxation rate peak can be recorded. In the case of cubic Li$_x$TiS$_2$ the SLR rate maximum appears at $T_{\max} = 515$ K for $\omega_0/2\pi = 19.2$ MHz. According to the maximum condition, $\omega_0 \tau \approx 1$, a mean Li jump rate τ^{-1} of about $1.2 \cdot 10^8$ s^{-1} is obtained at this temperature. In order to study slower translational Li motions some spin-lattice relaxation measurements in the rotating frame at effective locking frequencies in the kHz range were carried out [4]. In Fig. 3 the spin-lattice relaxation data obtained in the laboratory frame at 19.2 MHz are compared with the rates $1/T_{1\rho}$ recorded in the rotating reference frame at a locking frequency of about 2 kHz. As expected, reducing the resonance frequency raises the spin-lattice relaxation rate and shifts the diffusion induced rate maximum to lower temperatures. The $1/T_{1\rho}$ peak maximum shows up at $T_{\max} = 320$ K (Fig. 3). Using $\omega_1 \tau \approx 0.5$, which holds for the rotating frame case [26], a Li jump rate τ^{-1} of about $1.7 \cdot 10^4$ s^{-1} can be estimated. The corresponding relaxation rate peaks of hexagonal Li$_{0.7}$TiS$_2$ are shown in Fig. 4 for comparison. At comparable resonance and locking frequencies, respectively, the diffusion induced $1/T_1$ and $1/T_{1\rho}$ rate peaks of hexagonal Li$_{0.7}$TiS$_2$ are shifted to lower temperatures revealing that Li diffusion in the layered 2D host is significantly faster than that in the cubic modification. The slightly higher Li content of the hexagonal sample
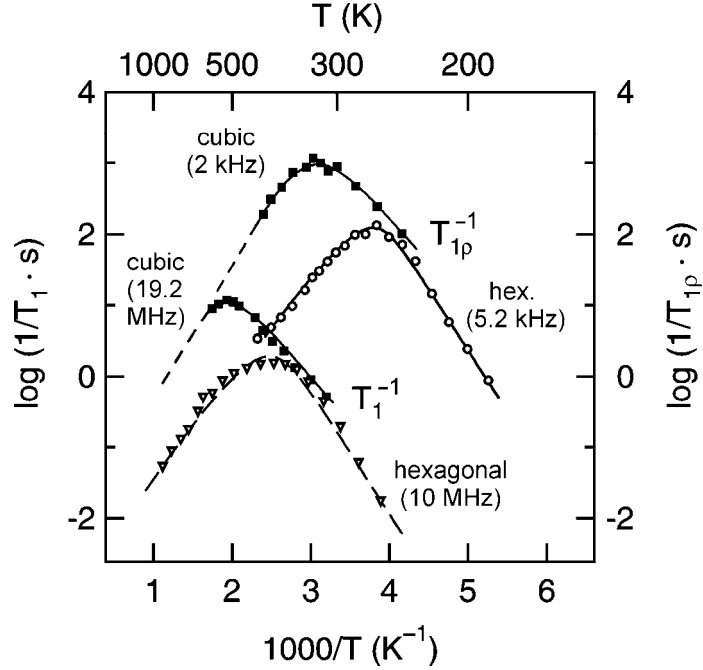
6

Fig. 3: Laboratory and rotating frame spin-lattice relaxation rates of cubic Li$_x$TiS$_2$ *vs* reciprocal temperature. Relaxation rates were recorded at a resonance frequency of 19.2 MHz and at a locking frequency of 2 kHz. The Larmor frequency of the rotating frame experiments was 77.8 MHz. Rotating frame data were taken from Refs. [12,24].

($x = 0.7$) compared to that of the cubic one ($x = 0.6$) does not impede this effect to be revealed because the maximum positions of a hexagonal sample with $x = 0.6$ would show an additional shift to lower temperatures, if at all.

The low-T slope of the $1/T_{1\rho}(1/T)$ peak of the cubic polymorph (Figs. 3 and 4) is similar to that of the corresponding $1/T_1(1/T)$ peak. The same is observed for hexagonal Li$_{0.7}$TiS$_2$: The activation energies of the low-T flanks of the $1/T_1$ and $1/T_{1\rho}$ data are similar (*cf.* Fig. 4). In contrast to the cubic polymorph the slopes of the high-T flanks of the $1/T_{1\rho}(1/T)$ and $1/T_1(1/T)$ relaxation peaks of the hexagonal modification are smaller by a factor of about 0.78 than those on the low-T side. The latter behaviour is due to 2D diffusion (see, *e. g.*, [26]) being present in hexagonal Li$_x$TiS$_2$. In the case of cubic Li$_{0.6}$TiS$_2$ the high-T flank of the $1/T_{1\rho}(1/T)$ peak corresponds to an activation energy of about 0.33 eV, thus, somewhat higher than that deduced from the low-T flank.

The detection of Li jump rates with values smaller than 10^4 s^{-1} would require locking frequencies below 1 kHz corresponding to locking fields of the order of 10^{-4} T. On the one hand, this can hardly be realized experimentally using the spin-lock technique. On the other hand, the lower limit of the locking field amplitude is given by the strength of

Fig. 4: Temperature dependence of laboratory and rotating frame spin-lattice relaxation rates of cubic $Li_{0.6}TiS_2$ and hexagonal $Li_{0.7}TiS_2$. Rotating frame data were recorded at about 2 kHz for cubic $Li_{0.6}TiS_2$ and at 5.2 kHz in the case of hexagonal $Li_{0.7}TiS_2$. The corresponding data in the laboratory frame were measured at 19.2 MHz (cubic) and 10 MHz (hexagonal), respectively. Data of the hexagonal modification were taken from Ref. [11].

local magnetic fields present in the sample itself. In the case of cubic $Li_{0.6}TiS_2$ local magnetic fields correspond to frequencies of the order of 1 kHz. Alternatively, smaller Li jump rates can be probed by recording [7]Li stimulated echoes (see section 3.3).

3.3 ^{7}Li stimulated echo NMR measurements: extremely slow Li jumps

[7]Li spin-alignment echo (SAE) NMR spectroscopy was used to trace extremely slow Li jumps with rates below 10^4 s^{-1}. Alignment echoes were recorded via the Jeener-Broekaert pulse sequence at a fixed evolution time t_p of 12 μs and for variable mixing times t_m. Echo amplitudes S_2 of c-$Li_{0.6}TiS_2$, which were read out at $t = t_p$, are shown in Fig. 5 vs t_m. Between $T = 170$ K and $T = 250$ K the S_2 decay curves can be parameterized with stretched exponentials according to $S_2 = S_\infty + S_\infty^0 \exp(-(\tau_{SAE}/t_m)^\gamma)$. Echo amplitudes were normalised to range between $S_\infty^0 = 0$ and $S_2^0 = 1$. The stretching exponent γ strongly depends on temperature and ranges from 0.6 to 0.1 between 173 K and 253 K. The corresponding decay constants τ_{SAE}^{-1} are shown in the Arrhenius plot of Fig. 6 to-

8
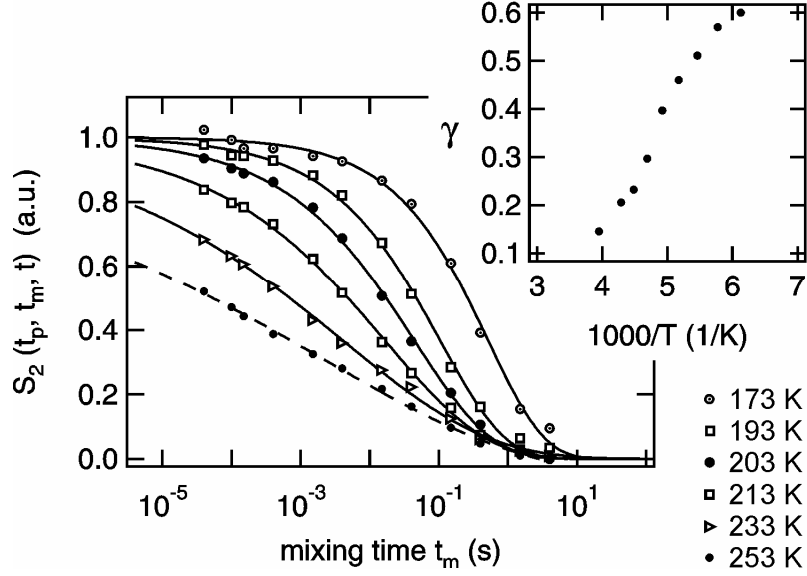
Fig. 5: [7]Li spin-alignment echoes of cubic $Li_{0.6}TiS_2$ as a function of mixing time. Data were recorded for fixed evolution time $t_p = 12$ μs and at 155 MHz. Between 173 and 253 K the decay curves follow stretched exponentials (fit curves shown). The inset displays the stretching exponents *vs* reciprocal temperature.

gether with those obtained by ^{7}Li spin-alignment echo NMR measurements on hexagonal $Li_{0.7}TiS_2$. For comparison, the $1/T_{1\rho}$ and $1/T_1$ data recorded at 2 kHz and 19.2 MHz, respectively, are shown again (*cf.* Fig. 3). Below 200 K the spin-alignment echo decay rates τ_{SAE}^{-1} of the cubic sample follow an Arrhenius law with a slope being similar to that obtained from the $1/T_{1\rho}$ measurements. Presumably, in this temperature range the spin-alignment echo decay is primarily induced by other spin-lattice relaxation processes. At temperatures above 200 K the stimulated echo decay is increasingly damped by an additional process characterized by a decay constant which we will identify with the ionic jump rate τ^{-1}, *i. e.*, $\tau^{-1} = \tau_{SAE}^{-1}$ (see below).

In Fig. 7 the Li jump rates obtained by ^{7}Li spin-alignment echo NMR are compared with those obtained from the maxima positions of the $1/T_{1\rho}(1/T)$ peaks recorded at different locking frequencies (*cf.* Fig. 4). Data points from both methods can be described with the same Arrhenius law characterized by an activation energy of 0.37(1) eV. Interestingly, this activation energy is very similar to that obtained for the hexagonal modification. For comparison, the Li jump rates of hexagonal $Li_{0.7}TiS_2$ are shown in Fig. 7, too. Obviously, in each of the two modifications the same diffusion process is detected by $1/T_{1\rho}$ relaxation NMR and ^{7}Li spin-alignment echo NMR. However, in the 3D host the Li diffusivity is reduced by about a factor of ten compared to that in the layered modifica-

9
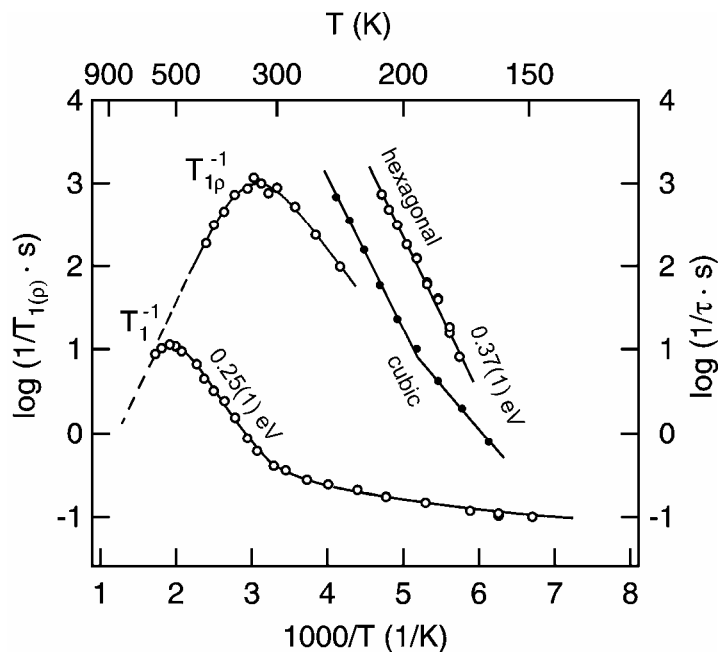
Fig. 6: Spin-alignment echo decay rates $1/\tau_{SAE}$ or Li jump rates $1/\tau$ (right-hand scale) of cubic $Li_{0.6}TiS_2$ *vs* reciprocal temperature. The rates were obtained from the SAE data in Fig. 5. For comparison the $1/T_{1\rho}$ and $1/T_1$ data (left-hand scale) of cubic $Li_{0.6}TiS_2$ from Fig. 3 as well as spin-alignment echo decay rates (right-hand scale) of hexagonal $Li_{0.7}TiS_2$, which were taken from Ref. [11], are also shown.

tion. A similar result was previously obtained by James and Goodenough [30] who measured the chemical diffusion coefficients of both polymorphs by galvanostatic and ac impedance methods. Regarding the local environment of a Li ion in the two materials this result is not surprising. In both modifications the Li ions preferentially occupy octahedral positions. In the case of layered titanium disulfide jumping of the cation between two octahedral sites involves the tetrahedral position to which the octahedra are connected by face-sharing.

Quite recently, this diffusion pathway has been experimentally probed by evolution time dependent ^{7}Li stimulated echo NMR spectroscopy [11,31]. Quantum chemical calculations on layered Li_xTiSe_2 also predict the involvement of tetrahedral sites in the diffusion process [32]. The fact that for the cubic form the Arrhenius plot yields practically the same activation energy indicates that below 400 K a similar (if not the same) elementary jump process is apparently present in the 3D host structure. This similarity of the two polymorphs was supposed before by Sinha and Murphy [10] as well as by Bruce and Saidi [33]. For the two modifications the interatomic distances of octahedral and tetrahe-

dral sites are very similar. Obviously, the dimensionality of the transport process is not due to a difference of the local energy barriers probed here but results from the pre-exponential factor of the corresponding Arrhenius law, which is reduced in the case of the cubic modification. The cubic polymorph can be derived from the hexagonal one when 1/4 of the titanium cations are shifted into the van-der-Waals gap where they occupy the same sites as Li. Thus, the structure of cubic Li_xTiS_2 may be thought of as having the same layered structure as hexagonal Li_xTiS_2 but with 1/4 of the interlayer Li sites occupied by Ti, see Ref. [10].

One should note that for layered TiS_2 the presence of excess Ti between the layers slows down intercalation considerably [1]. The "intralayer vacancies" in cubic Li_xTiS_2, which allow 3D diffusion, seem to not fully compensate for this slowing down at tem-
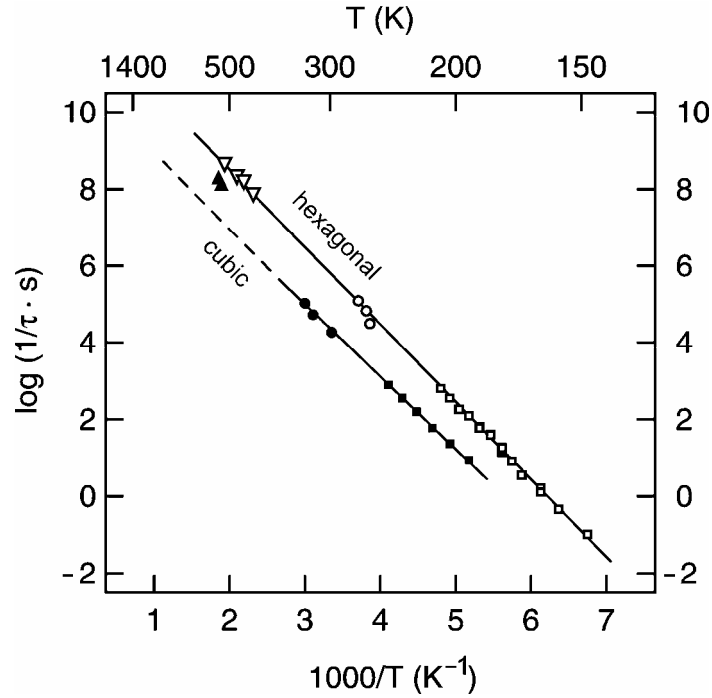
Fig. 7: Li jump rates of cubic and hexagonal lithium titanium disulfide. Values smaller than 10^{-4} s^{-1} were measured by recording ^{7}Li spin-alignment two-time correlation functions. In both cases (□: hexagonal $Li_{0.7}TiS_2$, ■: cubic $Li_{0.6}TiS_2$) stimulated echoes were recorded at 155 MHz. Li jump rates between 10^5 s^{-1} and 10^6 s^{-1} were determined from the diffusion induced relaxation rate maxima of $1/T_{1\rho}(1/T)$ recorded at different locking frequencies in the kHz range. Higher jump rates have been deduced from the maxima positions of diffusion induced $1/T_1(1/T)$ peaks at different Larmor frequencies in the MHz range. Data for hexagonal $Li_{0.7}TiS_2$ were taken from Ref. [11].

peratures below about 400 K. Whereas for hexagonal $Li_{0.7}TiS_2$ the jump rates, obtained from the frequency dependent spin-lattice relaxation measurements in both the laboratory and rotating frame, fit to the Arrhenius line shown in Fig. 7, the Li jump rates deduced from $1/T_1$ measurements for the cubic sample deviate from the temperature dependence extrapolated from the $1/T_{1\rho}$ and SAE NMR data. Presumably, additional Li jump processes take place at higher temperatures in the cubic polymorph which are absent in the layered one. Whereas the interlayer space in hexagonal Li_xTiS_2 is exclusively built up by face-shared octahedra and tetrahedra, in the cubic modification additional tetrahedral positions do exist. The increase of Li jump rates as deduced from the $1/T_1$ results for cubic $Li_{0.6}TiS_2$ is presumably due to additional Li hops between two octahedral positions without passing the tetrahedral site or/and due to the activation of other diffusion pathways.

Conclusion

Li diffusion in two host structures providing macroscopic diffusion pathways of different dimensionality but having practically the same chemical composition, *viz* cubic $Li_{0.6}TiS_2$ and hexagonal $Li_{0.7}TiS_2$, was investigated by solid state ^7Li NMR spectroscopy. Between 200 and 400 K the jump rates measured by ^7Li spin-alignment echo NMR and $T_{1\rho}$ relaxation NMR reveal an activation energy of about 0.37 eV for the two modifications indicating that the elementary jump process is similar in both polymorphs. However, the pre-exponential factor of the corresponding Arrhenius law of the cubic sample is reduced by about one order of magnitude. Obiously, Li diffusion in a 2D host structure is favoured compared to that in a 3D host system. At high temperatures in the cubic modification additional diffusion pathways seem to be relevant which do not show up in the hexagonal modification.

Acknowledgement

References

[1]   M. S. Whittingham, Prog. Solid State Chem. 12 (1978) 41.
[2]   M. S. Whittingham, A.J. Jacobson, Intercalation Chemistry, Academic Press, New York, 1982.
[3]   F. A. Levy, Intercalated Layered Materials, Reidel, Dordrecht, 1979.
[4]   W. Küchler, P. Heitjans, A. Payer, R. Schöllhorn, Solid State Ion. 70-71 (1994) 434.
[5]   A. F. McDowell, C. F. Mendelsohn, M. S. Conradi, R. C. Bowman (Jr.), A. J. Maeland, Phys. Rev. B 51 (1995) 6336.
[6]   M. S. Whittingham, Chem. Rev. 104 (2004) 4271
[7]   M. S. Wittingham, R. Chen, T. Chirayil, P. Zavalij, Solid State Ion. 94 (1997) 227.
[8]   M. Wilkening, P. Heitjans, Diffusion Fundamentals 2 (2005) 60.
[9]   R. Schöllhorn, A. Payer, Angew. Chem. Int. Ed. Engl. 24 (1985) 67.

[10] S. Sinha, D. W. Murphy, Solid State Ion. 20 (1986) 81.

[11] M. Wilkening, W. Küchler, P. Heitjans, Phys. Rev. Lett. 97 (2006) 065901.

[12] W. Küchler, P. Heitjans, D. Clausen, A. Payer, R. Schöllhorn, in: M. Mehring, J. U. von Schütz and H. C. Wolf (Eds.), 25th Congress Ampere on Magnetic Resonance and Related Phenomena, Springer-Verlag, Berlin, Heidelberg, New York, 1990.

[13] E. Fukushima, S. B. W. Roeder, Experimental Pulse NMR, Addison-Wesley, Reading, 1981.

[14] A. G. Redfield, Phys. Rev. 98 (1955) 1787.

[15] D. C. Ailion, C. P. Slichter, Phys. Rev. 137 (1965) A235.

[16] D. C. Look, I. J. Lowe, J. Chem. Phys. 44 (1966) 2995.

[17] F. Qi, G. Diezemann, H. Böhm, J. Lambert, R. Böhmer, J. Magn. Res. 169 (2004) 225.

[18] F. Qi, T. Jörg, R. Böhmer, Solid State Nucl. Magn. Res. 22 (2002) 484.

[19] J. Jeener, P. Broekaert, Phys. Rev. 157 (1967) 232.

[20] R. Böhmer, J. Magn. Res. 147 (2000) 78.

[21] K. Eichele, WSolids1, Version 1.17.30, Universität Tübingen, 2001.

[22] C. Prigge, W. Müller-Warmuth, Z. Phys. Chem. 189 (1995) 153.

[23] T. Bredow, P. Heitjans, M. Wilkening, Phys . Rev. B 70 (2004) 115111.

[24] W. Küchler, Ph.D. thesis, Universität Hannover, 1994.

[25] P. Heitjans, S. Indris, M. Wilkening, Diffusion Fundamentals 2 (2005) 45.

[26] P. Heitjans, A. Schirmer, S. Indris, in: P. Heitjans and J. Kärger (Eds.), Diffusion in Condensed Matter - Methods, Materials, Models, Springer, Berlin, 2005.

[27] M. Meyer, P. Maass, A. Bunde, Phys. Rev. Lett. 71 (1993) 573.

[28] K. L. Ngai, Comments Solid State Phys. 9 (1980) 141.

[29] K. Funke, Prog. Solid State Chem. 22 (1993) 111.

[30] A. C. W. P. James, J. B. Goodenough, Solid State Ion. 27 (1988) 37.

[31] M. Wilkening, Ph.D. thesis, Universität Hannover, 2005.

[32] C. Ramírez, R. Adelung, R. Kunz, L. Kipp, W. Schattke, Phys. Rev. B 71 (2005) 035426

[33] P.G. Bruce, M.Y. Saidi, Electrochimica Acta 36 (1991) 569.

[34] Y. Saidi, I. Abrahams, P. G. Bruce, Mat. Res. Bull. 25 (1990) 533.